Type of contribution:
Editorial
▶ Research Paper
Case Study
Review Paper
Scientific Data
Report of Tech. Application

e-issn. 2798-5245

Mechanical Engineering for Society and Industry
Vol. 4, No. 2 (2024) pp 177-197
https://doi.org/10.31603/mesi.12053

Modulating the holding time of hardening process in Q-P-T heat treatment: An experimental study on mechanical properties of medium-carbon steel plate

Alief Muhammad[1]*, Dani Hari Tunggal Prasetiyo[2], Poppy Puspitasari[3]

[1] Department of Mechanical Engineering, Universitas Panca Marga, Probolinggo 67216, **Indonesia**
[2] Department of Mechanical Engineering, Universitas Jember, Jember 68121, **Indonesia**
[3] Department of Mechanical and Industrial Engineering, Universitas Negeri Malang, Malang 68121, **Indonesia**
✉ im.m.alief@gmail.com

This article contributes to:

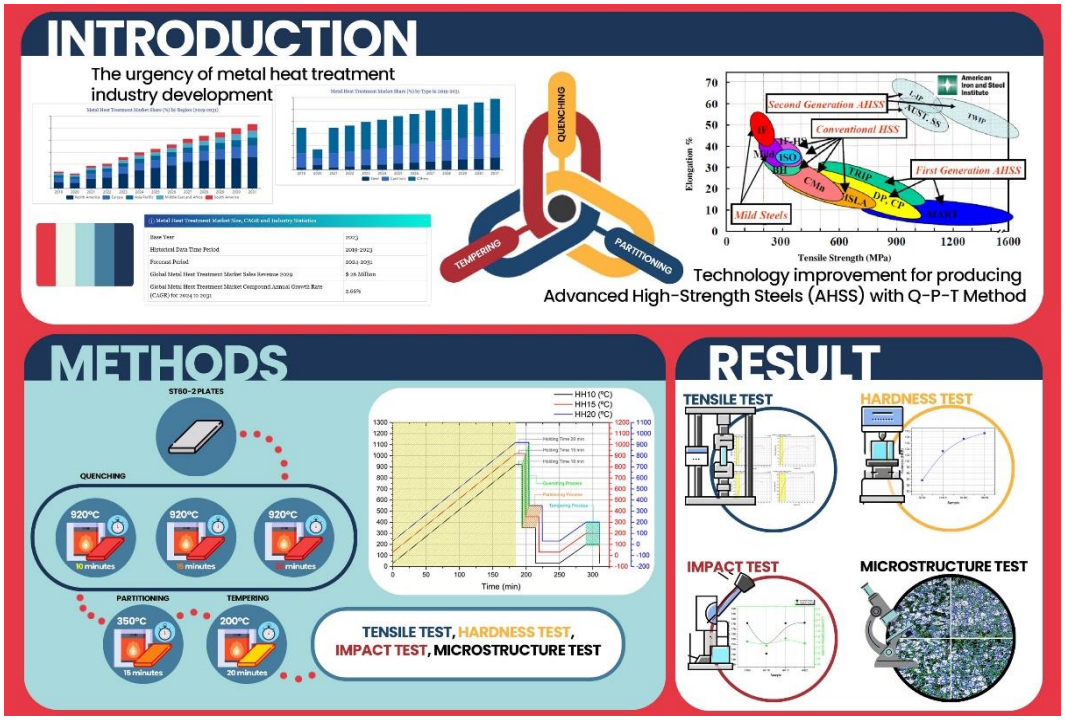

Highlights:

- Longer holding times in Q-P-T (10–20 minutes) improve tensile strength (74.02 kgf/mm²) and hardness (109.33 HRB).
- Q-P-T enhances medium-carbon steel through precise thermal treatment and phase transformation.
- Medium-carbon steel ST60-2 shows refined microstructure and better performance with extended holding times.

Article info
Submitted: 2024-08-07
Revised: 2024-11-20
Accepted: 2024-11-21

Publisher
Universitas Muhammadiyah Magelang

Abstract

The metal heat treatment industry has seen substantial growth, with market projections increasing by USD 15.18 billion from 2022 to 2027, driven by advancements in technology. The iron and steel industry significantly contributes to this growth, accounting for six percent of the market share. In this evolving landscape, the Quenching-Partitioning-Tempering (Q-P-T) technique is emerging as a valuable heat treatment process for enhancing Advanced High-Strength Steels (AHSS). The Q-P-T process, involving Quenching, Partitioning, and Tempering, aims to improve the mechanical properties of medium-carbon steels through controlled thermal modifications. This study explores the effects of varying holding times during the Q-P-T treatment on the mechanical properties and microstructure of medium-carbon steel ST60-2. Steel samples were subjected to holding times of 10, 15, and 20 minutes at a temperature of 920 °C, followed by quenching to 350 °C and partitioning at the same temperature for 15 minutes, with final tempering at 200 °C. The

results indicate that longer holding times enhance mechanical properties such as Ultimate Tensile Strength (UTS), Product of Strength and Elongation (PSE), and hardness, with the 20-minute sample (Sample 3) achieving the highest UTS of 74.02 kgf/mm² and elongation of 16.63%. Hardness peaked at 109.33 HRB, and improved toughness was observed due to better phase transformation and carbon partitioning (1.36 Joule/mm²). Microstructural analysis revealed finer and more uniformly distributed cementite particles with extended holding times, contributing to enhanced material performance. The findings underscore the potential of Q-P-T heat treatment in optimizing medium-carbon steels, offering a tailored approach for applications requiring superior mechanical properties.

Keywords: Q-P-T heat-treatment; Medium-carbon steel; Mechanical properties

1. Introduction

The metal heat treatment industry stands on the brink of significant growth, with market projections increasing by USD 15.18 billion from 2022 to 2027 [1]. Among the key players in this sector, the iron and steel industry hold a substantial share, contributing six percent to the entire heat treatment industry. As 2023 approaches, this sector is undergoing a transformative phase driven by cutting-edge technology. Some prominent trends include the integration of technologies such as artificial intelligence, automation, and robotics into heat treatment processes [2]–[6]. Furthermore, the integration of these advanced technologies could revolutionize the way metals are treated and processed before application across various fields. This advancement is expected to enhance efficiency, precision, and overall productivity in metal component manufacturing, fostering innovation across various industries [7], [8].

Amidst this dynamic landscape, there exists an emerging heat treatment technique deserving attention, namely the Q-P-T heat treatment [9]–[12]. The Q-P-T process involves three primary steps: hardening (Hardening-Quenching), partitioning, and tempering, each contributing to the final properties of the material. The Q-P-T (Quenching-Partitioning-Tempering) heat treatment on medium-carbon steel has garnered attention from materials experts and engineers due to its unique ability to enhance mechanical properties and material performance [13]–[15]. Medium-carbon steel generally exhibits a balanced combination of strength and toughness, making it a popular choice across various engineering applications.

The selection of medium-carbon steel (ST60-2) for this research, despite its common use without heat treatment for many applications, is motivated by its significant potential to achieve enhanced and tailored mechanical properties through controlled thermal processing. While medium-carbon steels are often employed as-is, numerous studies indicate that these materials can gain substantial performance benefits from specific heat treatments, making them suitable for specialized applications. Heat treatment can substantially alter the microstructure and mechanical behavior of medium-carbon steels like ST60-2. Processes such as annealing, normalizing, and hardening can improve mechanical properties such as tensile strength, hardness, and ductility [16]–[19]. For example, annealed samples of medium-carbon steel exhibit lower tensile strength and hardness but possess higher ductility, whereas hardened samples achieve superior tensile strength and hardness at the cost of reduced ductility. This property variability allows for precise optimization depending on application needs [20], [21].

The influence of heat treatment on the microstructure and mechanical performance of medium-carbon steels is well-documented. Parameters such as heating temperature, holding time, and cooling medium can lead to significant property enhancements. For instance, heating steels like S45C above 800 °C and cooling them in water substantially increases their hardness [22]. This demonstrates that controlled heat treatment offers the ability to tailor hardness and toughness in medium-carbon steels, making them adaptable for applications that demand specific mechanical properties.

The present study also illustrates how hardening ST60 steel under varying conditions can significantly increase surface hardness. For example, hardening at 1000 °C followed by water quenching produced a peak hardness of 112.73 HRB, while quenching in oil and saltwater yielded hardness values of 75.24 HRB and 88.50 HRB, respectively [23]. This underscores the potential of heat-treated ST60-2 to attain high deformation resistance due to martensitic transformation, which is particularly advantageous for wear-resistant applications requiring robust surfaces.

Further property enhancement can be achieved through tempering of hardened ST60 steel. Tempering at temperatures between 300 °C and 500 °C reduces residual stresses while maintaining a balance of hardness and ductility, resulting in improved toughness and greater suitability for

structural and mechanical applications [23]. This ability to fine-tune properties through heat treatment supports the use of ST60-2 steel, especially for applications that require controlled hardness and toughness.

Specialized heat treatment processes, such as austempering, further highlight the versatility of medium-carbon steels. Austempered ST60Mn steel demonstrates significant improvements in corrosion-wear resistance, evidenced by a substantial reduction in wear rate during testing in corrosive environments such as cassava juice [24]. This improvement shows that austempering can effectively optimize hardness and corrosion resistance, making medium-carbon steels suitable for components exposed to harsh conditions.

Medium-carbon steel components are widely utilized due to their balanced strength and ductility. However, as industrial demands for higher durability, reliability, and resistance to adverse conditions grow, enhancing the properties of these steels through heat treatment becomes essential. Techniques such as normalizing and annealing can homogenize the microstructure and enhance machinability or ductility while preserving adequate toughness [23]. The adaptability and optimization potential provided by these processes further justify the selection of ST60-2 steel for heat treatment research.

Based on previous research in steel heat treatment, the Q-P-T process has been employed in the application of Advanced High-Strength Steels (AHSS) to achieve good ductility and strength [25]–[28]. Research on Q-P-T had thus far yielded promising results in its mechanical properties. For instance, varying the deformation temperatures within the range of 25-350 °C in medium-carbon steel resulted in the highest Products of Strength and Elongation (PSE) of 5887.64 kgf/mm^2 % [29]. Similarly, adjusting the holding time partitioning between 5-90 minutes in high-carbon steel produced the highest PSE value of 3365.06 kgf/mm^2 % [30]. Another study involving holding time partitioning between 10-1000 seconds in medium-carbon steel revealed a maximum PSE value of 2422.85 kgf/mm^2 % [31]. These findings highlight the potential of Q-P-T in optimizing the mechanical properties of steel, emphasizing its efficacy in achieving desirable PSE values. This necessitates a broader exploration within Q-P-T to delve deeper into generating advanced high-strength steels (AHSS), particularly in the variations of holding time during the hardening-quenching process. This is because the hardening-quenching process plays a crucial initial role in enhancing the initial hardness of the material, especially in medium-carbon steel, which exhibits a more varied potential outcome. The initial role of hardening-quenching determines the enhancement of material elasticity without significantly compromising its hardness level.

The precise control of the Q-P-T steps enables the process to achieve an optimal balance between strength and toughness in the final material [32]–[35]. This makes it highly suitable for applications in the automotive, aerospace, and engineering industries. As the metal heat treatment industry continues to evolve and embraces advanced techniques like Q-P-T, the opportunities to enhance material performance and engineering applications become increasingly promising [36]–[39]. Therefore, in comprehensively understanding the mechanical property outcomes generated by the Q-P-T method, this research conducts an experimental study on the influence of hardening holding time within the Q-P-T method on medium-carbon steel.

In the metal industry, qualifying and characterizing the mechanical properties of metals become crucial factors in marketing and tailoring metal needs for applied applications [40]–[44]. Hence, mechanical testing is an important step in understanding the properties of materials after undergoing Q-P-T heat treatment on medium-carbon steel. Four common types of mechanical testing used are tensile testing, Rockwell hardness testing, impact Charpy testing, and microstructure testing.

Diligently conducting microstructure and mechanical tests, including tensile, Rockwell hardness, and impact tests, on medium-carbon steel after Q-P-T heat treatment, could provide profound insights into the mechanical properties of the material. These data are crucial in ensuring that the material meets specific application requirements and needs, thereby ensuring success and safety in its utilization across various industrial sectors.

2. Methods

2.1. Materials

In this research, an analysis of the mechanical properties of medium-carbon steel ST60-2 (with a chemical composition that could be seen in **Table 1**) processed using the Q-P-T heat treatment method was conducted. This study aims to comprehend how variations in holding time

during the hardening stage within the heat treatment combination could affect the phase transformation, strength, hardness, and toughness of this steel. The mechanical specifications of the initial material ST60-2 are detailed in **Table 2**, while the results of the mechanical tests for the untreated sample (Sample 0) are included in **Table 4** and serve as a baseline for comparison with all heat-treated samples. Additionally, the evaluation aims to assess its suitability for applications requiring high structural strength. The Q-P-T method involves three combination of heat treatment processes: Quenching, Partitioning, and Tempering. This research comprised three primary stages: sample preparation, sample testing, and analytical assessment.

Table 1. Chemical composition for ST60-2 steel plate (Product Analysis Max wt%) [45]

C	Si	Mn	P	S	N
0.40	0.60	1.70	0.06	0.06	0.01

Table 2. Mechanical Properties for ST60-2 steel plate [45]

Product Thicknesses (mm)	Tensile Strength (kgf/mm²)	Upper Yield strength (kgf/mm²)	Elongation (%)
<3	60.16	34.16	19 to 17
>3 to 100	58.12 to 72.40	33.14 to 30.08	16 to 12

2.2. Sample Preparation and Heat Treatment

The Temperature-Time diagram of the Q-P-T heat treatment, as shown in **Figure 1**, provides a detailed illustration of how temperature changes over time during the quenching, partitioning, and tempering process for three different samples. The x-axis represents the time in minutes, while the y-axes display temperature in degrees Celsius (°C), differentiated by three colors: black, red, and blue, corresponding to the three samples HH10, HH15, and HH20, respectively.

The black line on the graph depicts the temperature profile of sample HH10. This line illustrates how the sample undergoes quenching, partitioning, and tempering processes over time, with specific temperature changes along the black y-axis. Similarly, the red line represents the temperature variations of sample HH15, plotted against the red y-axis. It provides a distinct trajectory reflecting the time and temperature conditions specific to this sample. Finally, the blue line corresponds to sample HH20, where its temperature changes are mapped along the blue y-axis, demonstrating the thermal treatment applied to this sample.

Each line distinctly marks the critical stages of the Q-P-T heat treatment: the initial quenching from 920 °C to 350 °C, followed by partitioning at 350 °C, and concluding with tempering at 200 °C. The graph emphasizes the differences in holding times for quenching and the consistency of the partitioning and tempering temperatures across all samples. This visualization is essential for analyzing the thermal history and understanding its impact on the microstructure and mechanical properties of the medium-carbon steel samples.

The first stage involves sample preparation using the Q-P-T method, which consists of three processes, as shown in **Figure 1**. The initial process is quenching, where the steel sample is heated above its critical temperature, specifically at 920 °C. The specimens were heated in a controlled manner using Thermo Scientific Thermolyne Benchtop Muffle Furnaces FB1410M-33, a gas furnace system recognized for its accuracy and dependability in maintaining the desired thermal conditions. Thermal identification of the specimens was performed using the Seek Shotpro Thermal Imaging Camera, which offers precise thermal imaging capabilities crucial for evaluating temperature variations and thermal profiles. The material is held at this temperature for three different durations: 10 minutes, 15 minutes, and 20 minutes, as shown in **Table 3**. Subsequently, the material is rapidly cooled using SAE 15W-40 Oil as the quenching medium, not to room temperature, but to a temperature of 350 °C. The objective is to produce a structure that is not excessively hard but remains crack-resistant and sufficiently strong [46].

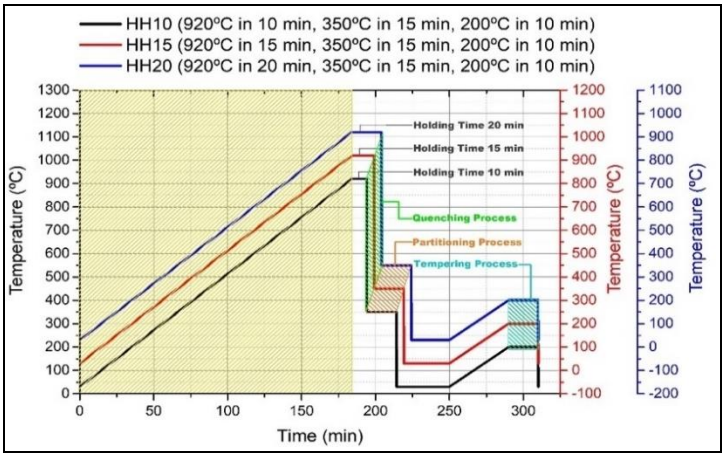

Figure 1. Temperature-Time diagram of Q-P-T heat treatment

Table 3. List of temperatures and holding times for all samples in the Q-P-T heat treatment

Sample Number	Sample Code	Quenching		Partitioning		Tempering	
		Hardening Temperature	Holding Time	Temperature	Holding Time	Temperature	Holding Time
0	ST60	-	-	-	-	-	-
1	HH10	920 °C	**10 min**	350 °C	15 min	200 °C	10 min
2	HH15	920 °C	**15 min**	350 °C	15 min	200 °C	10 min
3	HH20	920 °C	**20 min**	350 °C	15 min	200 °C	10 min

By swiftly cooling the metal only to an intermediate temperature, it retains some level of strength and hardness while reducing the risk of distortion and cracks that might occur with cooling to room temperature. This rapid cooling also allows the atoms in the material to lock into different crystal arrangements, resulting in a denser and harder structure [47].

During the partitioning process, the metal previously quenched to achieve a martensitic structure is altered to partition alloying elements into the matrix. This aims to enhance material properties, such as toughness and strength [48]. The partitioning process involves heating the material at a specific temperature lower than the quenching temperature, typically ranging between 350 °C to 450 °C [49], with this research employing a temperature of 350 °C for 15 minutes. At this temperature, the dissolved alloying elements within the matrix could diffuse and partition between the martensitic and austenitic phases (that has formed at a temperature of 920 °C), particularly during quenching as the material cools from 920 °C to 350 °C. This process could result in a more homogeneous structure with evenly distributed alloying elements [50]. The outcomes obtained from the partitioning process include increased hardness, toughness, and strength of the material, along with improved dimensional stability. Hence, partitioning stands as a critical step in optimizing material properties for applications that demand high strength and toughness.

Figure 2 illustrates thermal camera images that depict the temperature evolution during the heat treatment process, transitioning from 920 °C to 200 °C. The images are labeled as follows: (a) the sample at the quenching temperature of 920 °C, (b) the sample during the quenching stage cooled to 350 °C, and (c) the sample during the tempering process at 200 °C. On the right side of each image, a color contour is displayed, serving as a temperature indicator. The contour uses a gradient of colors where darker shades represent lower temperatures and lighter shades correspond to higher temperatures. It is important to note that the color ratios and the corresponding temperature values differ for each image. Consequently, each image has its own unique color scale and temperature indicator to accurately represent the thermal conditions at that specific stage of the heat treatment. Furthermore, green circles with numerical values are overlaid on the images. These points represent specific temperature measurements at precise locations on the sample. The numerical value within each green circle indicates the temperature recorded at that point, providing localized thermal data for the sample during each stage of the process. This combination of color contours and numerical temperature values offers a comprehensive visualization of the thermal profile of the samples, highlighting the changes in temperature distribution as they progress through the heat treatment process.

The final process of the Q-P-T method is Tempering, a crucial process in heat treatment following quenching and partitioning, aimed at restoring some of the strength and toughness that may have been affected by rapid cooling. In this stage, the metal is reheated to a lower temperature than the quenching temperature, typically ranging between 150 °C to 250 °C, depending on the material type and application requirements, with this research employing a temperature of 200 °C for 10 minutes. The primary goal of the tempering process is to reduce internal stresses that might have occurred during quenching and achieve an appropriate balance between hardness and toughness in the material [51].

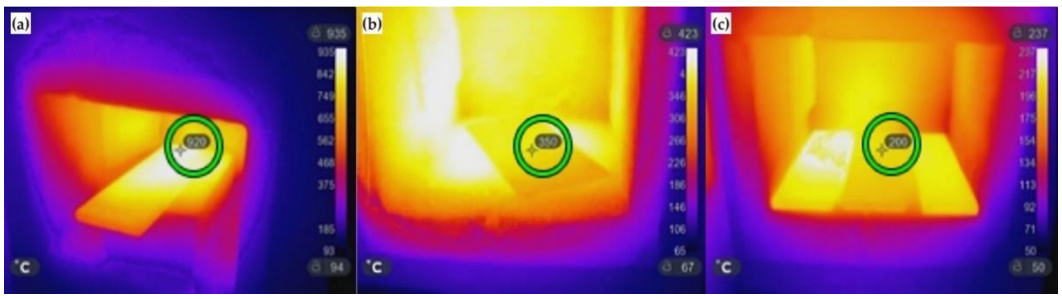

Figure 2. Sample temperature evolution during heat treatment: (a) Quenching temperature of 920 °C; (b) Quenching stage cooled to 350 °C; (c) Tempering process at 200 °C

During tempering, several changes occur in the material's structure, including phase transformations and redistribution of alloying elements. The outcome of tempering is an increase in the material's ductility, implying greater resistance to breakage and cracking [52]. Mechanical properties such as strength and hardness usually experience a decrease, but this is carefully controlled to achieve the desired balance between strength and toughness.

2.3. Mechanical Testing and Microstructure Analysis

The second stage involves testing, encompassing four types of tests: tensile testing, hardness testing, impact testing, and microstructure analysis. Each variation of the sample is tested three times for each test, and the average value of these test results is taken. Data resulting from tensile testing could provide a comprehensive understanding of the material's behavior under various loading conditions using ASTM A370 dimension standard, as shown in **Figure 3**. Tensile test results often include the yield point, ultimate tensile strength, elastic modulus, and elongation at fracture. This information can be used to assess the material's strength, toughness, elasticity, and ability to withstand specific loads without failure. Tensile test results play a crucial role in product design and development, ensuring that the materials used meet required standard specifications and safety criteria [54]. Tensile testing was conducted using a TARNO hydraulic universal tensile testing machine, a robust and versatile system designed to precisely measure the mechanical properties of materials under tension.

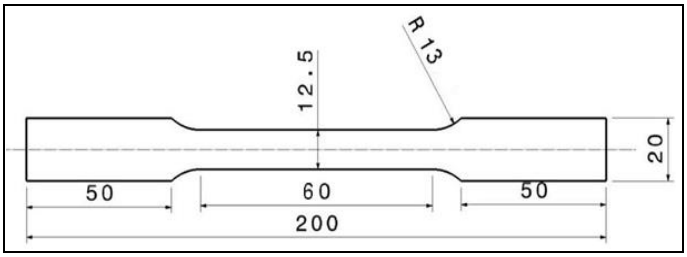

Figure 3. Sample of uniaxial test according ASTM A370 [53]

The subsequent test is hardness testing, involving applying a test load onto the material surface using a cone or ball-shaped penetrator made of hard materials like diamond or hardened steel. In this research, the specific type of hardness test used is the Rockwell hardness test. Hardness testing was carried out at specific points on the samples using the CARSON MOPAO3 M22011907 hardness tester. During the Rockwell hardness test, the penetrator is placed on the material surface with a predetermined initial load. Then, the load is incrementally increased in several stages, and at each stage, the depth of penetration of the penetrator into the material is measured. After the measurements, the results are recorded on the Rockwell scale, indicating the material's hardness level. The advantage of Rockwell hardness testing lies in its ability to deliver consistent and replicable results, along with its user-friendly nature [55].

The third test is the Charpy impact test, involving a predetermined heavy hammer dropped from a specific height to strike a V-shaped material sample with standardized size and geometry. In this study, the Charpy impact test used the RESIL IMPACTOR SNI ISO/IEC 17025 with the testing size standards conform to ASTM E23, as shown in **Figure 4**. These samples typically feature a specified notch to ensure consistent impact points. During the Charpy impact test, the energy absorbed by the material sample upon impact is measured as the height of the resulting fracture. The higher the fracture height, the lower the material's toughness. Results from the Charpy impact test are often expressed in joules. This test aims to evaluate the mechanical properties of materials used in applications that might experience impact loads, such as construction and structural engineering [56]. Data from this test assist in ensuring that the material could withstand potential impact loads during its use.

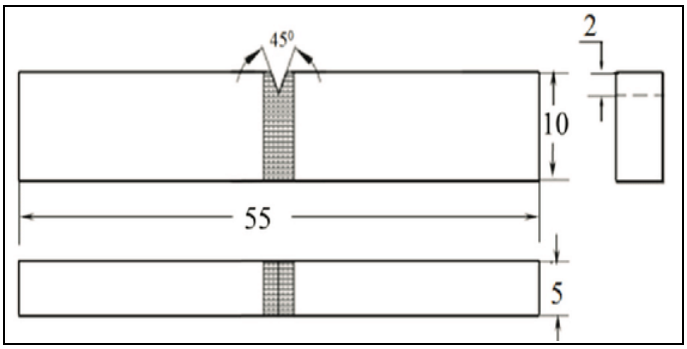

Figure 4. Temperature-Time diagram of Q-P-T heat treatment

The fourth test is microstructure testing, an analytical process to study the microscopic structure of steel metal. It involves observing and characterizing the metal's microstructure at an extremely small scale, such as metal grains, phases, and other features not observable to the naked eye. The primary aim of conducting microstructure testing on steel metal is to understand its Microstructure. Microstructure phase identification was performed using an Insize Metallurgical Microscope 5102-M600, which provides superior magnification capabilities of up to 200×. This test aids in comprehending the metal grain structure, phase distribution, and other microscopic

structures that influence the mechanical and physical properties of the material. Additionally, microstructure testing is performed to identify metal Components and Phases. In steel, microstructure testing assists in identifying the existing phases, such as ferrite, pearlite, or cementite, to confirm the strength, resilience, and other properties of the steel [57].

3. Results and Discussion

3.1. Tensile Strength

In this research, sample 1 was held for 10 minutes, sample 2 for 15 minutes, and sample 3 for 20 minutes. Subsequently, quenching was performed using oil until the temperature dropped to 350 °C, followed by the partitioning process at 350 °C for 15 minutes. Finally, tempering was conducted by heating all samples to 200 °C for 10 minutes and then cooling them with oil to reach room temperature. Each variation of the sample was tested three times, and the average value of these test results was taken.

Sample 0, a shown in **Figure 5**, exhibited a maximum tensile force of 2241.5 kgf, while sample 3 achieved the highest value at 2656 kgf. There was a significant increase in tensile force with an increase in holding time. Longer holding times at the hardening temperature resulted in steel with higher tensile strength. Sample 0 had a UTS of 59.96 kgf/mm^2, whereas sample 3 demonstrated the highest UTS at 74.02 kgf/mm^2. Similar to the tensile force results, UTS also increased with longer holding times, indicating stronger mechanical properties in ST60 steel.

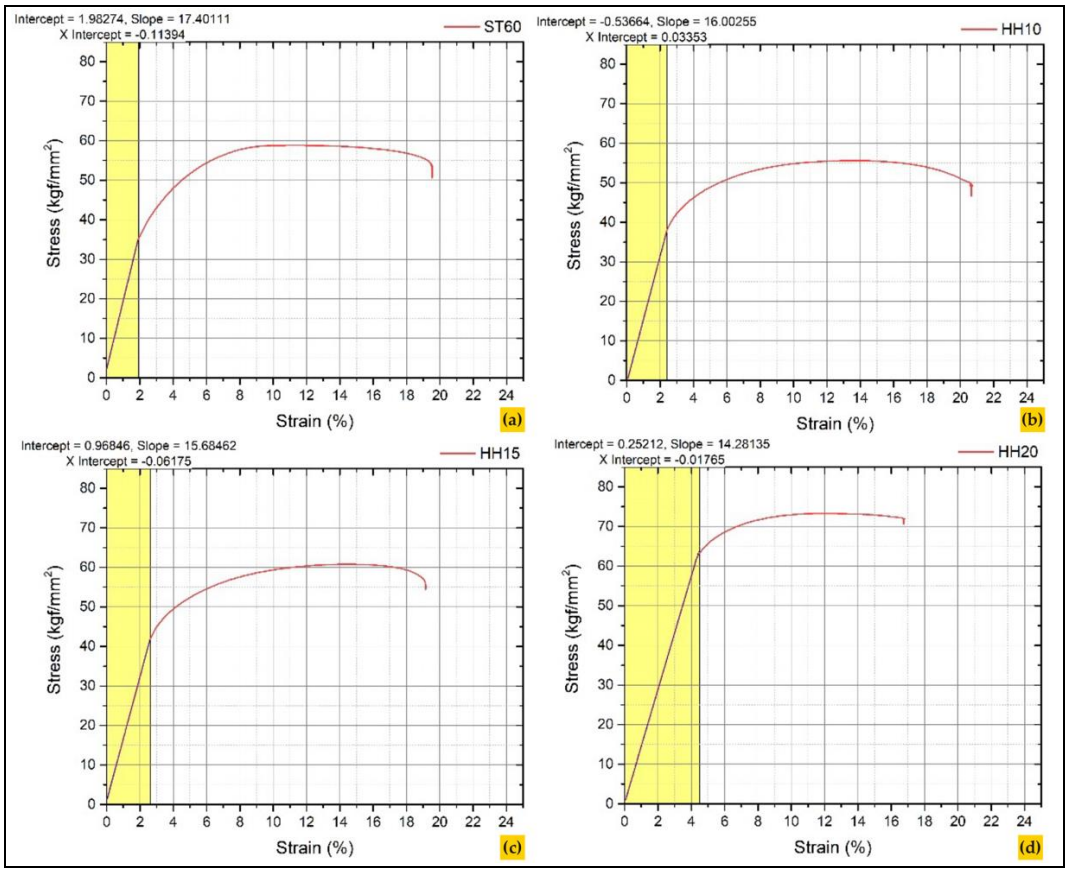

Figure 5. Stress-strain curves show distinctive characteristics across samples; (a) ST60 untreated sample; (b) HH10 sample with 10-minute holding time; (c) HH15 sample with 15-minute holding time; (d) HH20 Sample with 20-minute holding time

Sample 1 (held for 10 minutes during the Q-P-T heat treatment process) exhibits a lower Ultimate Tensile Strength (UTS) of 55.34 kgf/mm² compared to the untreated raw material, which has a UTS of 59.96 kgf/mm². This unexpected reduction in UTS is likely due to insufficient holding time at the hardening temperature of 920 °C. The phase transformation process from ferrite/pearlite to austenite during heating was not fully completed within the 10-minute duration [58]–[60]. As a result, the structure did not achieve a uniform or fully transformed austenitic phase, which is crucial for forming martensite upon quenching.

The incomplete austenite transformation leads to a less optimal martensitic structure during the quenching step [61], [62]. Additionally, inadequate carbon diffusion and partitioning during the subsequent partitioning phase at 350 °C may have further limited the enhancement of the steel's

strength. This is supported by the observation that extended holding times (as in Samples 2 and 3) result in significantly higher UTS values, with Sample 3 reaching a peak UTS of 74.02 kgf/mm².

Moreover, the rapid cooling during quenching might have introduced residual stresses or microstructural inconsistencies in Sample 1, reducing its mechanical performance. These factors collectively explain why Sample 1 does not show the expected increase in UTS typically associated with heat treatments conducted at temperatures above 900 °C. This highlights the critical role of holding time in ensuring the effectiveness of heat treatment processes.

When compared to other studies, the UTS results align with established findings that heat treatment significantly enhances the strength of medium-carbon steels. For instance, in the other study, the UTS of 0.25–0.35 grade medium-carbon steel ranged from 383.84 N/mm² (39.14 kgf/mm²) in the as-rolled condition to 621.2 N/mm² (63.34 kgf/mm²) after hardening at 900 °C [63]. This improvement reflects the influence of elevated temperatures on phase transformation, where austenite forms and subsequently transforms into martensite during rapid cooling, significantly increasing strength. The findings from this study demonstrate that the Q-P-T process for ST60 steel achieves comparable enhancements in UTS relative to similar grade steels hardened at 900 °C.

Additionally, insights from other related studies reported peak UTS values of 892 N/mm² (91 kgf/mm²) when using an optimized blend of vegetable oils as the quenching medium [64]. Although the UTS of ST60 steel in the current study peaked at 74.02 kgf/mm², differences in alloy composition and quenching mediums explain the variations. The blend of oils in the referenced study may have resulted in a more efficient quenching process, enabling higher tensile strengths.

It is also noteworthy that the UTS of 0.25–0.35 grade medium-carbon steel from the Nigeria study dropped from 1320 N/mm² (134.69 kgf/mm²) at 250°C tempering to 819 N/mm² (83.48 kgf/mm²) at 600 °C tempering [63]. This indicates the critical balance between hardening and tempering temperatures in achieving an optimal combination of strength and ductility. For ST60 steel, tempering at 200 °C after partitioning ensured a moderate reduction in brittleness while maintaining high tensile strength, showcasing the suitability of the Q-P-T process for applications requiring superior mechanical properties and structural reliability.

Overall, the comparison highlights the effectiveness of the Q-P-T heat treatment in enhancing UTS, though specific results depend on factors such as alloy composition, quenching medium, and precise heat treatment parameters. The findings underscore the versatility of the Q-P-T method in optimizing the mechanical properties of medium-carbon steels for tailored industrial applications.

As the steel is heated to the hardening temperature (920 °C), a phase transformation occurs. At this temperature, the austenitic phase forms from the existing steel phase structure. Longer holding times provide more time for a more complete transformation into the austenitic phase [65]. This yields a more homogeneous structure, consequently enhancing tensile strength. Extended holding times facilitate more extensive atom diffusion within the steel's microstructure. Atoms within the material move and diffuse to more optimal positions, forming stronger atomic bonds. This could result in a denser and stronger structure [66].

The partitioning process at 350 °C for 15 minutes enables atom segregation and carbon partitioning within the microstructure of the steel [67]. The holding time during the partitioning process allows for better carbon partitioning into the martensitic phase, significantly increasing the hardness and strength of the steel. Longer holding times facilitate more carbon partitioning into the martensitic phase, further enhancing the hardness and strength of the material.

The yield strength of ST60 steel subjected to Q-P-T heat treatment shows a notable enhancement compared to the untreated condition. The untreated sample exhibited a yield strength of 34.69 kgf/mm², as shown in **Table 4**. In contrast, heat-treated samples demonstrated increased values: 36.62 kgf/mm² (10-minute holding time), 41.06 kgf/mm² (15-minute holding time), and a maximum of 63.35 kgf/mm² (20-minute holding time). This improvement can be attributed to the extended holding time at the hardening temperature of 920 °C, facilitating a more complete transformation into the austenitic phase and better carbon partitioning during the partitioning process at 350 °C. These factors contribute to a denser and more homogeneously distributed martensitic structure, which enhances the yield strength. Longer holding times resulted in higher yield strength, as shown in **Figure 6**, indicating the steel's greater ability to withstand loads without permanent deformation. As the steel is heated to a high hardening temperature, a phase transformation occurs from the initial structure to the austenitic phase. Longer holding times

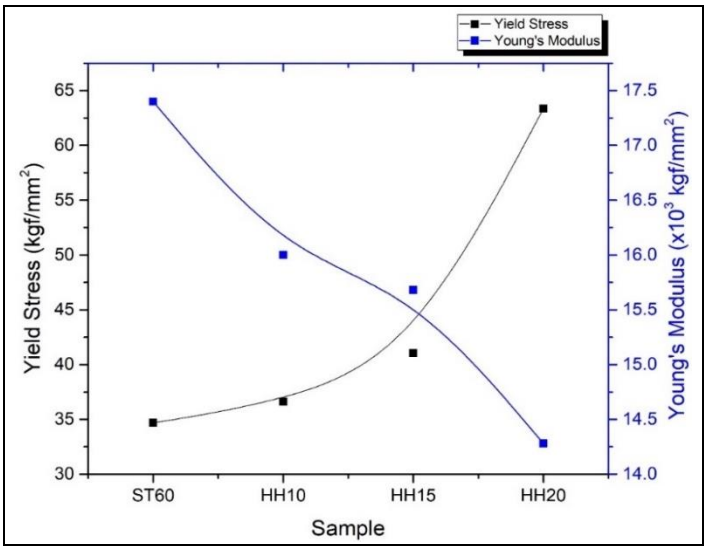

Figure 6. A comparative graph of yield strength and young's modulus

allow for a more complete phase transformation. The austenitic phase is typically more homogeneous and has a denser structure compared to the initial structure [27], which could result in steel with higher yield strength.

In comparison, the other study highlights that annealed specimens of medium-carbon steel achieved a yield strength of 45.87 kgf/mm² (450 MPa), the highest among tested specimens, while normalized samples exhibited the lowest yield strength of 22.43 kgf/mm² (220 MPa) [68]. This aligns with the observed impact of specific heat treatment processes on the mechanical properties of medium-carbon steels. The ST60 steel's performance in this study, with a yield strength of up to 63.35 kgf/mm², demonstrates the superior outcomes of the Q-P-T method over standard annealing or normalizing techniques.

Table 4. Summarizing tensile test outcomes for all samples

Sample Number	Sample Code	Max. Force (kgf)	Average UTS (kgf/mm²)	Average Yield strength (kgf/mm²)	Average Elongation (%)	Average Young's Modulus (x10³ kgf/mm²)	Average PSE (kgf/mm² %)
0	ST60	2241.5	59.96	34.69	19.51	17.40	1169.82
1	HH10	2050	55.34	36.62	20.36	16.00	1126.72
2	HH15	2125	61.91	41.06	19.24	15.68	1191.15
3	HH20	2656.5	74.02	63.35	16.63	14.28	1230.95

Furthermore, findings from the other study reveal that hardened samples achieved a yield strength of 42.01 kgf/mm² (412.10 MPa), which decreased to 29.57 kgf/mm² (290 MPa) when tempered at 250 °C and further to 22.17 kgf/mm² (217.31 MPa) at 450 °C [69]. While hardening initially increases yield strength, tempering reduces it as temperature rises due to the relaxation of internal stresses and partial phase transformation. The Q-P-T-treated ST60 steel demonstrates a balanced approach, retaining higher yield strength even after tempering at 200 °C, underscoring the advantages of controlled partitioning and tempering steps in preserving strength. These comparisons highlight that while standard hardening and tempering can enhance yield strength, the Q-P-T process offers a tailored approach to achieve higher yield strength, making it particularly advantageous for applications requiring robust mechanical performance and structural integrity.

The measurement of modulus of elasticity across the four samples revealed significant differences in values, as shown in **Figure 6**. Sample 0 exhibited the highest modulus of elasticity at 17.40*10³ kgf/mm², whereas Sample 3 registered the lowest value at 14.28*10³ kgf/mm². Modulus of elasticity denotes the material's stiffness before permanent deformation occurs. Within the scope of this research, there's an observable trend indicating that longer holding times lead to a decrease in the modulus of elasticity. This phenomenon indicates that prolonged holding times may render the material more pliable before reaching the point of permanent deformation [70].

The measurement results of elongation in the four samples showed varying figures. The elongation values of ST60 steel subjected to Q-P-T heat treatment reveal significant variations based on holding times during the hardening process, shown on **Figure 7**. The untreated sample exhibited an elongation of 19.51%, which increased to 20.36% for Sample 1 (10-minute holding time) but decreased to 19.24% for Sample 2 (15-minute holding time) and 16.63% for Sample 3 (20-minute holding time). The higher elongation observed in Sample 1 is attributed to the shorter holding time, which resulted in a less fully transformed martensitic structure, thereby retaining some ductility [9]. Conversely, the extended holding times in Samples 2 and 3 led to a denser and more uniform martensitic phase, which improved strength at the cost of reduced ductility.

In comparison, the other study reports elongation values of 26–47% for medium-carbon steel processed under optimal heat treatment conditions, including an intercritical heating temperature of 850°C and a cooling rate of 30 °C/s [71]. These conditions facilitated the retention of 16% austenite, contributing to both high strength and significant elongation. The ST60 steel elongation

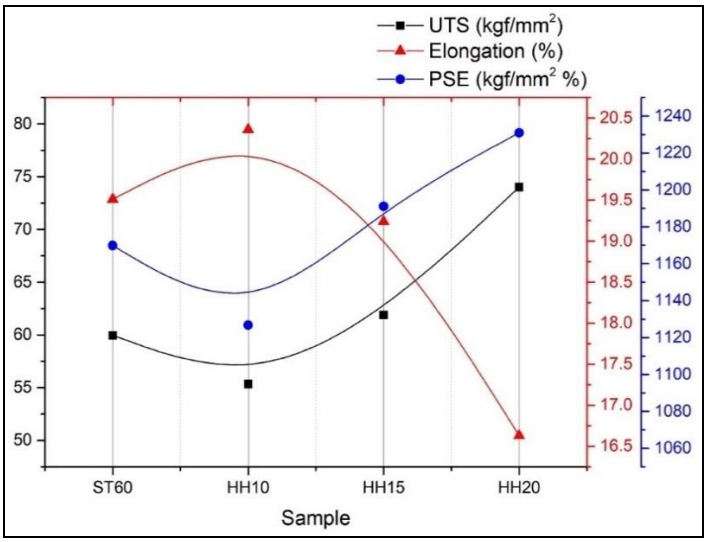

Figure 7. Graphical comparison of UTS, elongation, and PSE among samples

values, although lower, reflect the specific effects of the Q-P-T process, where the partitioning and tempering stages prioritized enhancing strength over retaining significant ductility.

Furthermore, insights from other research suggest that oil quenching generally results in higher elongation compared to water quenching [72]. For instance, mild steel quenched in oil at 100 °C, 300 °C, and 500 °C exhibited elongation values of 18.5%, 14.1%, and 12.4%, respectively, while water-quenched samples showed lower elongation values of 16.7%, 12.3%, and 9.8% [72]. In the current study, the use of oil as the quenching medium for ST60 steel similarly helped preserve elongation, especially for Sample 1. However, as the holding time increased, the more complete phase transformation and martensitic structure reduced elongation due to increased brittleness. These findings underscore the balance achieved by the Q-P-T heat treatment process in tailoring mechanical properties. While elongation decreases with longer holding times due to the dominance of the martensitic phase, the ductility of Sample 1 highlights the potential of shorter holding times for applications requiring greater elongation and moderate strength.

The measurement results of the Product of Strength and Elongation (PSE) in the four samples provided significant insights, as shown in **Figure 7**. Sample 3, subjected to a holding time of 20 minutes, recorded the highest PSE value at 1230.95 kgf/mm^2 %, while Sample 1 exhibited the lowest value at 1126.72 kgf/mm^2 %. PSE values depict the level of strain when the material begins to fracture. In this context, an increase in holding time correlates with an increase in PSE values. This effect is notably observed in Sample 3, experiencing an extended holding time, signifying that the material underwent greater plastic strain before reaching its fracture point. These findings illustrate the significant impact of holding time in heat treatment on the level of plastic strain exhibited by materials before structural failure occurs [73].

The tensile testing results indicate that varying holding times in the Q-P-T heat treatment could result in significant changes in the mechanical properties of ST60 steel. Longer holding times lead to steel with higher tensile strength, Ultimate Tensile Strength (UTS), yield strength, and modulus of elasticity, albeit with lower elongation. Essentially, longer holding times during the hardening phase provide opportunities for a more complete phase transformation process, microstructure refinement, and strengthening of atomic bonds within the material, ultimately resulting in steel with higher tensile strength [74]. Therefore, these findings are supported by changes in the microstructure and properties that occur during the heat treatment, allowing the steel to withstand mechanical loads more effectively.

3.2. Hardness Strength

The data indicates an increase in hardness values with an increase in holding time, as shown in **Table 5**. Sample 0, which did not undergo specific heat treatment, had an initial hardness value of approximately 93.67 HRB, while samples with longer holding times (samples 1, 2, and 3) showed significantly higher hardness values. Sample 3, with the longest holding time (20 minutes), reached the highest hardness value of around 109.33 HRB, as shown in **Figure 8**. When comparing these results with the other study it is noted that the maximum hardness for medium carbon steel reached 58 HRC after hardening at 900 °C, which is equivalent to approximately 56.9 HRB [69]. The hardness decreased as tempering temperatures increased: from 53 HRC (51.2 HRB) at 250 °C to 39 HRC (38.3 HRB) at 550 °C. This decrease in hardness with increasing tempering temperatures aligns with the findings from this study, where longer holding times at high temperatures allowed for a more complete transformation, which enhanced hardness but also could lead to a reduction in ductility.

Increasing the holding time during heat treatment allows for more thorough transformation of the austenitic phases and facilitates better carbon partitioning within the steel's microstructure.

When the steel is held at elevated temperatures, the austenitic phase stabilizes, and more carbon atoms dissolve into it. As a result, upon cooling, a larger amount of carbon can be incorporated into the martensitic phase, which forms during rapid cooling. This higher carbon content in the martensitic structure leads to a denser and harder material because carbon atoms hinder dislocation movement, increasing the overall hardness of the steel [75]. Thus, extending the holding time enhances the transformation process and significantly contributes to the improved hardness of the final steel product.

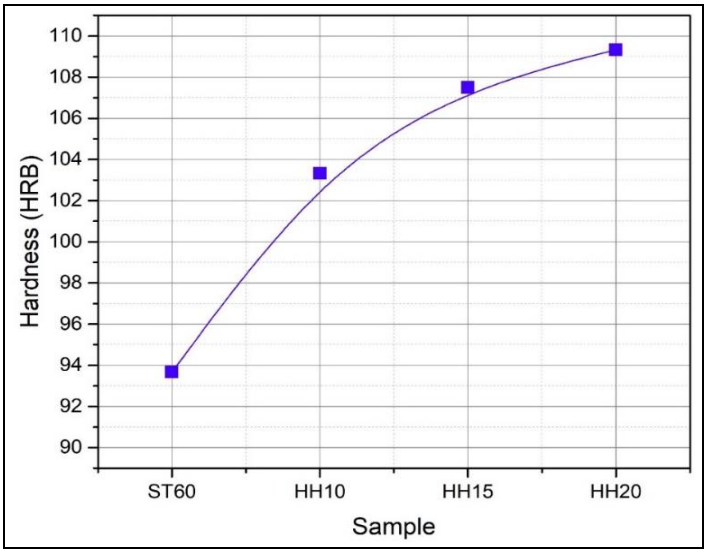

Figure 8. Hardness value distribution across various samples

Table 5. Summarized list of hardness values for all samples

Sample Number	Major Load (kgf)	Minor Load (kgf)	Duration (s)	Indentor	HRB
0	100	10	5	Steel Ball 1/6	93.67
1	100	10	5	Steel Ball 1/6	103.33
2	100	10	5	Steel Ball 1/6	107.5
3	100	10	5	Steel Ball 1/6	109.33

A longer holding time also allows more extensive atom diffusion within the steel's microstructure, which could strengthen atomic bonds and result in a harder material. The increase in hardness signifies an enhancement in the material's stiffness [76]. Therefore, the results indicate that longer holding times at the hardening temperature yield ST60 steel that is harder and more rigid. ST60 steel subjected to longer heat treatment holding times could be used in applications requiring components with high hardness. Overall, the Rockwell hardness test results indicate that longer holding times at the hardening temperature contribute to increased hardness in ST60 steel, enhancing its stiffness for applications requiring stronger mechanical properties.

3.3. Impact Strength

Sample 0 exhibited an actual energy value of 175.94 Joules, as shown in **Table 6**. This indicates that the ST60 steel sample, without undergoing heat treatment, possesses high toughness, necessary to absorb significant impact energy before fracturing or experiencing substantial damage. Sample 3 showcased the highest actual energy value among the samples with different holding times, reaching 176.18 Joules. This suggests that a longer holding time at the 920°C hardening temperature enhances the toughness of the sample, requiring more energy to break it. Sample 1 displayed the lowest actual energy value among the samples with varying holding times, recording 145.8 Joules. This demonstrates that a shorter holding time, in this case, 10 minutes, results in lower toughness.

Table 6. Detailed list of impact values across all samples

Sample Number	Sample Code	Actual Energy (Joule)	Specific Impact (Joule/mm²)
1	ST60	175.94	1.43
2	HH10	145.8	1.28
3	HH15	175.84	1.54
4	HH20	176.18	1.36

In comparison to the other study where the impact toughness of heat-treated medium carbon steel (38MnVS6) was reported to have improved with a Charpy impact energy of approximately 25 J, similar to the impact energies observed for ST60 steel in the current study [77]. The enhancement in impact toughness for both studies can be attributed to the controlled quenching that induced bainitic or martensitic microstructures, thereby improving toughness compared to conventional heat treatment methods. Furthermore, more study reveals that medium carbon steel specimens treated at 900°C and cooled in a furnace achieved the highest impact energy of 20 J, while those quenched in water displayed a lower value of 6.2 J [78]. This suggests that slower cooling methods,

such as furnace cooling, enhance impact resistance by promoting microstructures that improve the material's ability to absorb energy during impact. The Q-P-T treatment applied to ST60 steel, which includes both quenching and partitioning phases, likely benefits from a similar phenomenon, where controlled cooling and partitioning result in improved toughness and resistance to impact, particularly in the samples with longer holding times. Thus, the impact energy results for ST60 steel reflect the effectiveness of the Q-P-T heat treatment in enhancing toughness while maintaining strength. The ability to balance these properties through precise control of quenching and partitioning times underscores the suitability of this treatment for applications requiring both high impact resistance and mechanical strength.

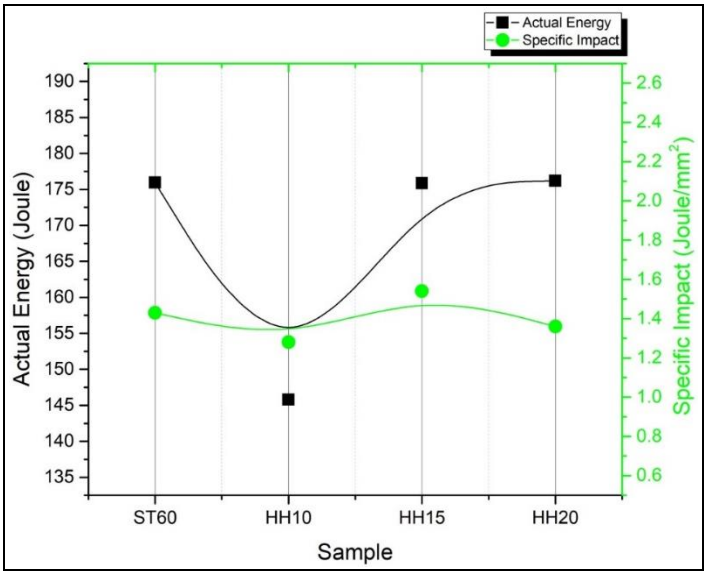

Figure 9. Graphical comparison of impact values and specific impact energy for all samples

Sample 2 attained the highest specific impact value, namely 1.54 Joules/mm^2. This value indicates that sample 2 efficiently absorbs impact energy within a specific surface area, as shown in **Figure 9**. The 15-minute holding time at the hardening temperature seems to enhance the sample's ability to absorb energy more efficiently. Sample 0 displayed a specific impact value of 1.43 Joules/mm^2, indicating good toughness in the untreated sample. This means that despite its high actual energy, its ability to absorb energy within a specific surface area is also quite commendable [79]. Sample 1 showed a specific impact value of 1.28 Joules/mm^2, suggesting that the 10-minute holding time at the hardening temperature results in slightly lower energy absorption capability within a specific surface area.

In this analysis, it could be concluded that the holding time during the heat treatment at the hardening temperature of 920°C has a significant impact on the toughness of the ST60 steel samples. Longer holding times appear to enhance the toughness of the samples, reflected in higher actual energy values. However, the specific impact values don't consistently follow the same pattern, indicating that toughness depends not only on the actual absorbed energy but also on the sample's ability to absorb energy within a specific surface area unit.

3.4. Microstructure Analysis

Microstructural tests were carried out and phase mapping was carried out, as shown in **Figure 10**. Ensure that the images are of high quality and accurately represent the microstructure of the samples. In this research, the captured images are imported into JMat Pro image analysis software. Use image processing tools to enhance contrast, adjust brightness, and remove any artifacts or noise that may interfere with the analysis. Utilize the software's tools to identify and distinguish between ferrite and pearlite phases within the microstructural images. This involves applying filters or thresholding techniques to isolate specific features characteristic of each phase. The presence of ferrite is mapped and marked with a blue line, while the presence of pearlite is mapped and marked with a green line. Once the phases are identified, quantify the percentage of ferrite and pearlite present in each image. This can be achieved by manually delineating regions corresponding to each phase or using automated segmentation algorithms to partition the image into distinct phase regions. The percentage of ferrite and pearlite is then calculated by dividing the area occupied by each phase by the total area of the microstructural image.

Sample 0 has an average grain diameter of 3.96 µm, ranging from 0.83 µm to 13.23 µm. The standard deviation of 2.34 indicates a fairly significant variation in the metal grain size, as shown in **Table 7**. Sample 1, with a holding time of 10 minutes, shows a decrease in the average diameter to 3.25 µm, ranging from 0.81 µm to 12.21 µm. The standard deviation of 1.74 indicates a lower variation compared to Sample 0. Sample 2, with a holding time of 15 minutes, demonstrates an increase in the average grain diameter to 3.79 µm, ranging from 0.83 µm to 12.64 µm. The standard deviation of 2.14 indicates a re-increase in variation. Sample 3, with a holding time of 20 minutes, shows a slight decrease in the average diameter to 3.39 µm, ranging from 0.82 µm to 12.00 µm.

The standard deviation of 1.89 indicates a relatively lower variation compared to Sample 2, as shown in **Figure 11**.

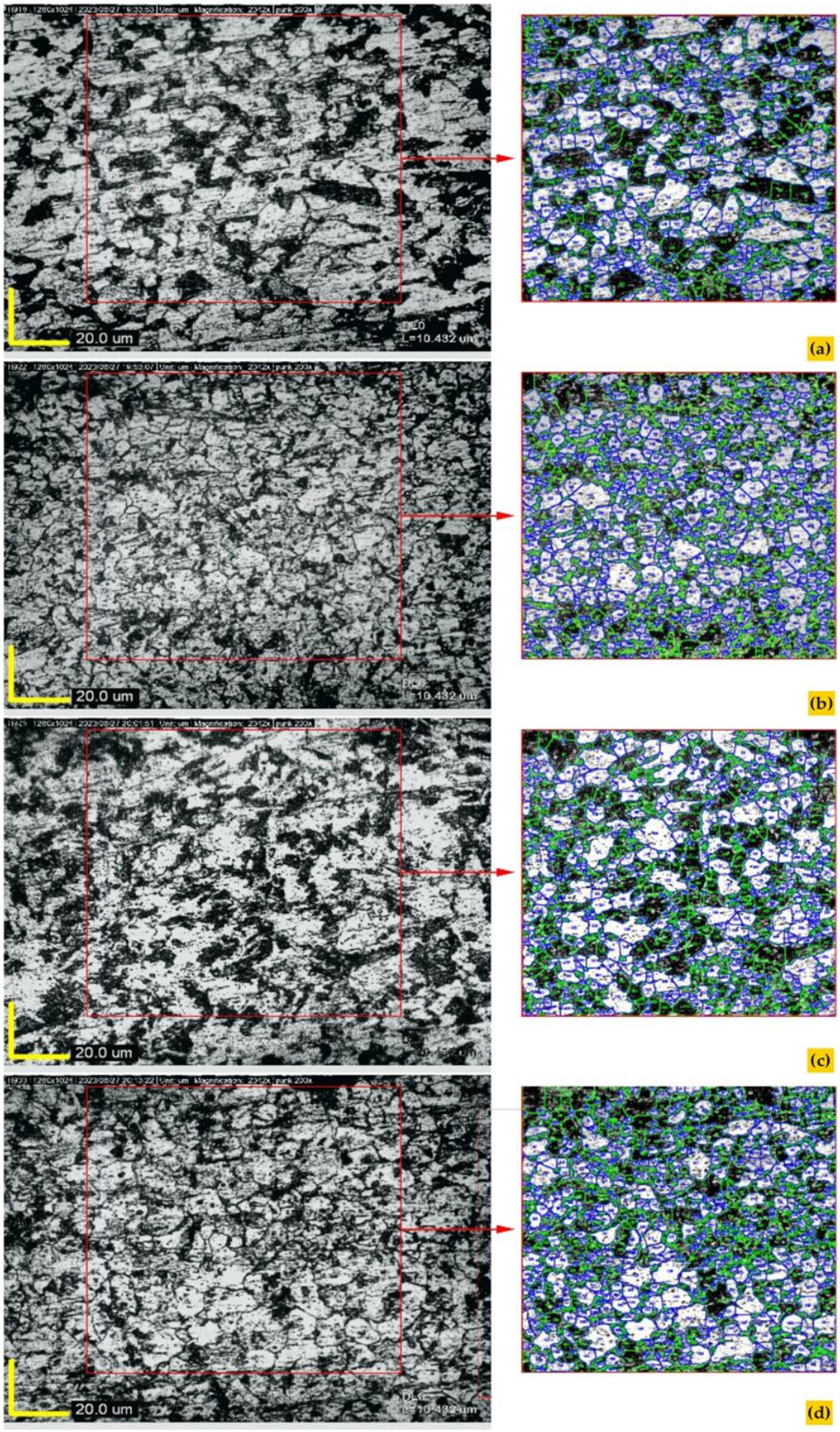

Figure 10. Detailed microstructural images with phase mapping across different samples: (a) ST60 untreated sample; (b) HH10 sample with 10-minute holding time; (c) HH15 sample with 15-minute holding time; (d) HH20 sample with 20-minute holding time

Table 7. Detailed list of microstructural key parameters across all samples

Sample Number	Mean Diameter (µm)	Minimum Diameter (µm)	Maximum Diameter (µm)	Standar Deviation (µm)	Area of Pearlite (%)	Area of Ferrite (%)
0	3.96	0.83	13.23	2.34	45.42	54.58
1	3.25	0.81	12.21	1.74	45.36	54.64
2	3.79	0.83	12.64	2.14	49.38	50.62
3	3.39	0.82	12	1.89	48.84	51.16

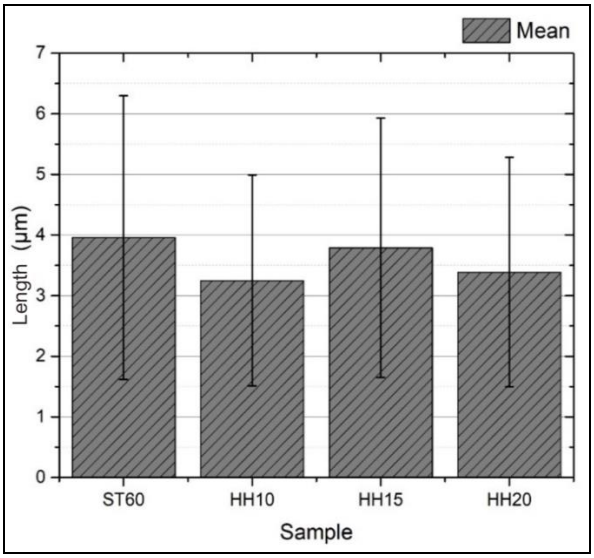

Figure 11. Graphical comparison of impact values and specific impact energy for all samples

The histograms analyzed illustrate the distribution of microstructure diameters for the all samples, as shown in **Figure 12**. For sample 0, the histogram reveals a peak count around 2-3 µm, with a right-skewed distribution extending up to approximately 12 µm and a maximum count of about 160. In contrast, sample 1 shows a similar peak diameter but with a higher maximum count of around 270-280 and a distribution tail extending to about 10 µm. Sample 2 also peaks around 2-3 µm and exhibits a right-skewed distribution with a tail reaching beyond 12 µm, though its maximum count is similar to sample 0 at approximately 160-170. Sample 3, on the other hand, has a peak count at 2-3 µm with a distribution tail extending beyond 12 µm and a maximum count falling between the values for sample 1 and the other samples, around 260-270. Overall, all samples display a right-skewed distribution of microstructure diameters, with peak diameters consistently in the 2-3 µm range. Notably, sample 1 and sample 3 show higher counts compared to sample 0 and sample 2, and the distribution tails of sample 2 and sample 3 extend further, indicating a greater range of larger diameters.

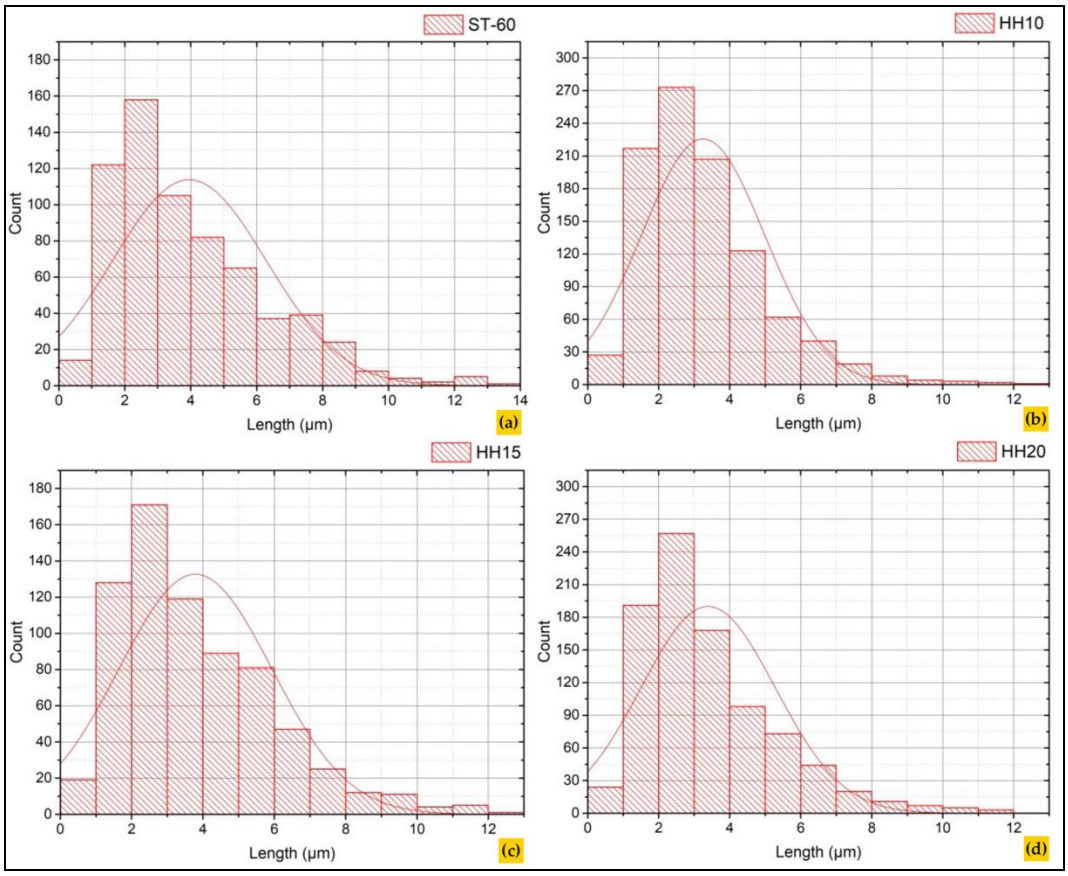

Figure 12. Histogram illustrating the diameters of microstructures in various samples: (a) ST60 Untreated sample; (b) HH10 Sample with 10-minute holding time; (c) HH15 Sample with 15-minute holding time; (d) HH20 Sample with 20-minute holding time

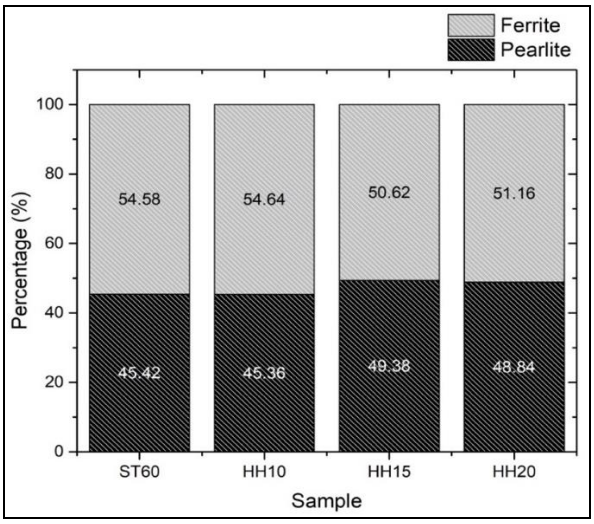

Figure 13. Graphical comparison of ferrite and pearlite area percentages across different samples

In Sample 0, the percentage area of the perlite phase is around 45.42%, while the ferrite phase constitutes about 54.58%, as shown in **Figure 13**. The sample subjected to a 10-minute holding time shows minimal changes in phase distribution, with percentages nearly similar to Sample 0. Sample 2, with a holding time of 15 minutes, increases the percentage of the perlite phase to 49.38% and the ferrite phase to 50.62%. Meanwhile, Sample 3, subjected to a 20-minute holding time, exhibits a slight decrease in the percentage of the perlite phase to 48.84% and an increase in the ferrite phase to 51.16%.

Different holding times in the heat treatment process exhibit a significant influence on the metal grain size and phase distribution [80]. Decreasing holding time seems to have a positive effect on the metal grain size with a lower standard deviation, indicating better consistency in the distribution of metal grain sizes. Holding time variations also affect the distribution of perlite and ferrite phases, which could impact the mechanical and structural properties of ST60-2 metal.

The comprehensive analysis of microstructural findings from the heat treatment of microalloyed medium-carbon steel reveals intricate relationships between the thermal processing conditions and resulting mechanical properties [77]. The microstructures analyzed predominantly consist of tempered martensite near the surface and a mixture of bainite, pearlite, and intergranular ferrite within the core. Notably, the tempered martensite formation is likely influenced by rapid cooling rates near the surface, enhancing hardness and wear resistance. The volume fractions of pearlite observed in the samples varied, with cylinder IV containing approximately 50% pearlite, contrasting with cylinders II and III, which exhibited around 30%, as shown on **Figure 14** [77]. This distribution suggests that the cooling rate significantly impacts pearlite formation, aligning with insights highlighting slower cooling as a contributor to higher pearlite fractions. The remaining core microstructure is dominated by bainitic structures, known for their balance of strength and toughness, further optimized by controlled cooling.

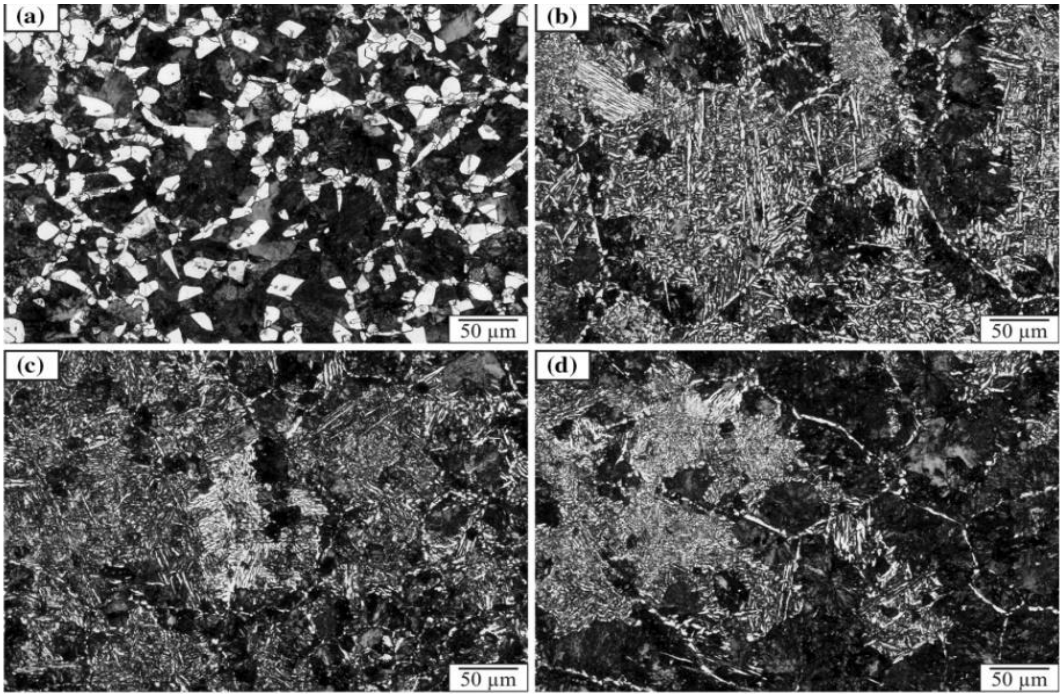

Figure 14. Optical micrographs of the heat treatment of microalloyed medium-carbon steel of the microstructure in the core regions of the cylinders: (a) I; (b) II; (c) III; and (d) IV [77]

Intragranular ferrite formation around manganese sulfide (MnS) precipitates is particularly noteworthy, as these structures nucleate on vanadium nitride (VN) surfaces [77]. This phenomenon underscores the role of microalloying elements in refining grain structure and

improving mechanical properties. The controlled cooling process, which varies in rate, is critical in tailoring the proportions of ferrite and pearlite, directly influencing the mechanical performance of the steel. These findings emphasize the intricate interplay between heat treatment parameters, microstructure evolution, and mechanical outcomes. The precise manipulation of thermal cycles, especially the cooling rates, enables the development of steel with tailored properties, making it suitable for high-strength applications while maintaining durability.

4. Conclusion

There's a significant increase in tensile strength with an extended holding time. Longer holding times during the hardening process result in steel with higher tensile strength. Similar to the tensile results, the UTS also increases with extended holding times, indicating stronger mechanical properties in ST60 steel. This is due to a more complete phase transformation, improved carbon partitioning, and a denser crystal structure. Longer holding times lead to higher yield strength, showcasing the steel's ability to withstand loads without permanent deformation. This is attributed to more complete phase transformations, improved carbon partitioning, and a stronger structure. However, longer holding times reduce the steel's ability to stretch before fracture. A more complete phase transformation and denser structure result in less elasticity in the steel. Longer holding times decrease the stiffness of the steel due to changes in phase, carbon partitioning, and the solidification of crystal structures, leading to a more elastic material.

Longer holding times result in increased hardness, driven by more complete phase transformations, enhanced carbon partitioning, extensive atom diffusion, and solidification of the microstructure. Extended holding times enhance toughness, reflected in higher actual energy values. However, specific impact values don't always follow the same pattern, indicating that toughness relies not only on the absorbed actual energy but also on the sample's ability to absorb energy within a specific surface area unit.

Sample 0 displays a significant variation in grain size, indicated by the high standard deviation. Different holding times exhibit diverse variations in the metal's grain size. Lower holding times tend to reduce the average grain size with a lower standard deviation. Alterations in holding time affect the phase distribution. A 15-minute holding time increases the percentage of pearlite phase, while a 20-minute holding time results in a slight decrease in the percentage of pearlite phase. Variations in holding time during the heat treatment affect the microstructural properties of the metal. Reduced holding times show better consistency in the distribution of grain sizes. Changes in the distribution of pearlite and ferrite phases could impact the mechanical and structural properties of ST60-2 metal.

Hence, the research findings indicate that holding time during the Q-P-T heat treatment significantly impacts the mechanical properties and toughness of ST60 steel. Longer holding times at a hardening temperature of 920 ºC have a positive effect on the strength, toughness, and resistance to plastic deformation of ST60 steel. Factors contributing to these outcomes include more complete phase transformation, improved carbon partitioning, and alterations in the microstructure.

Authors' Declaration

Authors' contributions and responsibilities - The authors made substantial contributions to the conception and design of the study. The authors took responsibility for data analysis, interpretation, and discussion of results. The authors read and approved the final manuscript.

Funding – No funding information from the authors.

Availability of data and materials - All data is available from the authors.

Competing interests - The authors declare no competing interest.

Additional information – No additional information from the authors.

References

[1] M. Phagare, "Metal Heat Treatment Market Report 2024 (Global Edition)," 2023.

[2] A. Adel, "Future of Industry 5.0 in Society: Human-Centric Solutions, Challenges and Prospective Research Areas," *Journal of Cloud Computing*, vol. 11, no. 1, 2022, doi:

10.1186/s13677-022-00314-5.

[3] M. Javaid, A. Haleem, R. P. Singh, R. Suman, and E. S. Gonzalez, "Understanding the Adoption of Industry 4.0 Technologies in Improving Environmental Sustainability," *Sustainable Operations and Computers*, vol. 3, no. September 2021, pp. 203–217, 2022, doi: 10.1016/j.susoc.2022.01.008.

[4] H. Liu, S. Dhawan, M. Shen, K. Chen, V. Wu, and L. Wang, "Industry 4.0 in Metal Forming Industry Towards Automotive Applications: A Review," *International Journal of Automotive Manufacturing and Materials*, vol. 1, Dec. 2022, doi: 10.53941/ijamm0101002.

[5] W. Setiawan, N. Santoso, W. Wiyadi, M. S. Aji, R. Alamin, and A. Tarmudi, "Lap Joint on St.37 Steel Plate with Friction Welding Clamping Method," *Journal of Mechanical Engineering Science and Technology (JMEST)*, vol. 7, no. 1, p. 47, 2023, doi: 10.17977/um016v7i12023p047.

[6] Y. R. A. Pradana, R. Afrianto, C. H. A. Rahman, and A. Andoko, "The Effect of Cutting Speed of Nitrogen Laser Cutting on the Surface Texture of SUS 304 Plate," *Journal of Mechanical Engineering Science and Technology (JMEST)*, vol. 7, no. 1, p. 66, 2023, doi: 10.17977/um016v7i12023p066.

[7] T. S. Amosun, S. O. Hammed, A. M. G. De Lima, and I. Habibi, "Effect of quenching media on mechanical properties of welded mild steel plate," *Mechanical Engineering for Society and Industry*, vol. 3, no. 1, pp. 4–11, Sep. 2022, doi: 10.31603/mesi.7121.

[8] K. Khoirudin *et al.*, "A Report on Metal Forming Technology Transfer from Expert to Industry for Improving Production Efficiency," *Mechanical Engineering for Society and Industry*, vol. 1, no. 2, pp. 96–103, Nov. 2021, doi: 10.31603/mesi.5613.

[9] Y. Peng, C. Liu, and N. Wang, "Effect of Deformation on Microstructure and Mechanical Properties of Medium Carbon Steel During Heat Treatment Process," *Chinese Journal of Mechanical Engineering (English Edition)*, vol. 34, no. 1, 2021, doi: 10.1186/s10033-021-00634-8.

[10] R. Zhao, T. Liu, and X. Zhao, "Effect of Q-P-T Process on the Microstructure and Mechanical Properties of 300M Steel," *Materials Science Forum*, vol. 749, pp. 287–293, Mar. 2013, doi: 10.4028/www.scientific.net/MSF.749.287.

[11] S. Qin *et al.*, "Approach and Mechanism of Toughness Enhancement for a High Carbon Q-P-T Steel," *Heat Treatment and Surface Engineering*, vol. 1, no. 1–2, pp. 11–16, 2019, doi: 10.1080/25787616.2018.1560160.

[12] H. Zheng, K. M. Wu, O. Isayev, O. Hress, S. Yershov, and V. Tsepelev, "Effect of Nb and Cu on the microstructure and hardness of quenching–partitioning–tempering dual-phase steels," *Heat Treatment and Surface Engineering*, vol. 1, no. 1–2, pp. 78–82, Apr. 2019, doi: 10.1080/25787616.2018.1560171.

[13] J. Dong, X. Zhou, Y. Liu, C. Li, C. Liu, and H. Li, "Effects of Quenching-Partitioning-Tempering Treatment on Microstructure and Mechanical Performance of Nb-V-Ti Microalloyed Ultra-High Strength Steel," *Materials Science and Engineering: A*, vol. 690, pp. 283–293, 2017, doi: 10.1016/j.msea.2017.03.020.

[14] D. Dong, H. Li, K. Shan, X. Jia, and L. Li, "Effects of Different Heat Treatment Process on Mechanical Properties and Microstructure of Q690 Steel Plate," *IOP Conference Series: Materials Science and Engineering*, vol. 394, no. 2, pp. 1–6, 2018, doi: 10.1088/1757-899X/394/2/022017.

[15] Y. Rong, "Quenching–Partitioning–Tempering (Q–P–T) Process and its Combination of Other Processes," *Heat Treatment and Surface Engineering*, vol. 1, no. 1–2, 2019, doi: 10.1080/25787616.2018.1560129.

[16] B. Shin, K. Kim, S. Yi, S. Choi, and S. Hyun, "Microstructure and Mechanical Properties of Cast and Hot-Rolled Medium-Carbon Steels under Isothermal Heat-Treatment Conditions," *Metals*, vol. 11, no. 12, p. 1950, Dec. 2021, doi: 10.3390/met11121950.

[17] N. M. Ismail, N. A. A. Khatif, M. A. K. A. Kecik, and M. A. H. Shaharudin, "The effect of heat treatment on the hardness and impact properties of medium carbon steel," *IOP Conference Series: Materials Science and Engineering*, vol. 114, no. 1, pp. 0–9, 2016, doi: 10.1088/1757-899X/114/1/012108.

[18] T. Protasenko, O. Rebrova, and H. Fedorenko, "Studying the influence of heat treatment

modes on the properties of medium-carbon steel," *Bulletin of Kharkov National Automobile and Highway University*, vol. 1, no. 103, p. 144, Dec. 2023, doi: 10.30977/BUL.2219-5548.2023.103.1.144.

[19] Y. D. B. A. Puraditya, D. D. Mahendra, and P. H. Setyarini, "Characteristics of Bio-ceramic Coating on Corrosion Rate of Stainless Steel 316L and Titanium (Ti-6Al-4V)," *Mechanics Exploration and Material Innovation*, vol. 1, no. 1, pp. 20–26, Jan. 2024, doi: 10.21776/ub.memi.2024.001.01.3.

[20] R. Suresh, "Investigation of Heat Treatment on Mechanical Properties of Medium Carbon Steel," *International Journal of Scientific Research in Science, Engineering and Technology*, vol. 8, no. 6, pp. 90–95, Dec. 2021, doi: 10.32628/IJSRSET21868.

[21] S. R. Harisha, S. Sharma, U. A. Kini, and M. C. Gowri Shankar, "Study on Spheroidization and Related Heat Treatments of Medium Carbon Alloy Steels," *MATEC Web of Conferences*, vol. 144, p. 02008, Jan. 2018, doi: 10.1051/matecconf/201814402008.

[22] P. T. Hang, "Effects of Heat Treatment Process on Mechanical Properties of Medium Carbon Steel," *Vietnam Journal of Agricultural Sciences*, vol. 4, no. 4, pp. 1283–1292, Dec. 2021, doi: 10.31817/vjas.2021.4.4.07.

[23] M. Nasution, "Engineering of St 60 Steel for Industrial Use with Tensile Test at PTKI Material Lab," *International Journal of Research and Review*, vol. 9, pp. 784–792, 2022, doi: 10.52403/ijrr.20220866.

[24] M. Bodude, W. Ayoola, D. Esezobor, and A. Agbeleye, "Corrosion-Wear of ST60-Mn Steel in Cassava Juice," *Journal of Minerals and Materials Characterization and Engineering*, vol. 11, 2012, doi: 10.4236/jmmce.2012.112012.

[25] A. Inam *et al.*, "Effect of Tempering Time on Microstructure, Mechanical, and Electrochemical Properties of Quenched-Partitioned-Tempered Advanced High Strength Steel (AHSS)," *Materials Research Express*, vol. 6, no. 12, 2019, doi: 10.1088/2053-1591/ab52b7.

[26] A. K. Singh, D. K. Chouhan, B. Bhattacharya, and S. Biswas, "High strength-ductility combination by quenching and partitioning of a low carbon microalloyed dual-phase steel," *Materials Science and Engineering: A*, vol. 870, p. 144854, Apr. 2023, doi: 10.1016/j.msea.2023.144854.

[27] D. Chatterjee, "Behind the Development of Advanced High Strength Steel (AHSS) Including Stainless Steel for Automotive and Structural Applications-An Overview," *Materials Science and Metallurgy Engineering*, vol. 4, no. 1, pp. 1–15, 2017, doi: 10.12691/msme-4-1-1.

[28] G. Y. Li, M. T. Ma, X. P. Mao, and C. X. Zhao, "New Process of Hot Stamping in Combination with Q-P-T Treatment for Higher Strength-Ductility Auto-Parts," *Advanced Materials Research*, vol. 1063, pp. 223–231, 2015, doi: 10.4028/www.scientific.net/AMR.1063.223.

[29] K. Zhang, M. Zhu, B. Lan, P. Liu, W. Li, and Y. Rong, "The Mechanism of High-Strength Quenching-Partitioning-Tempering Martensitic Steel at Elevated Temperatures," *Crystals*, vol. 9, no. 2, 2019, doi: 10.3390/cryst9020094.

[30] Z. li Tan, K. kai Wang, G. hui Gao, X. lu Gui, B. zhe Bai, and Y. qing Weng, "Mechanical Properties of Steels Treated by Q-P-T Process Incorporating Carbide-Free-Bainite/Martensite Multiphase Microstructure," *Journal of Iron and Steel Research International*, vol. 21, no. 2, pp. 191–196, 2014, doi: 10.1016/S1006-706X(14)60029-7.

[31] T. Y. Hsu, X. J. Jin, and Y. H. Rong, "Strengthening and Toughening Mechanisms of Quenching-Partitioning-Tempering (Q-P-T) Steels," *Journal of Alloys and Compounds*, vol. 577, no. SUPPL. 1, pp. S568–S571, 2013, doi: 10.1016/j.jallcom.2012.02.016.

[32] J. Zhang *et al.*, "Revealing Carbide Precipitation Effects and Their Mechanisms During Quenching-Partitioning-Tempering of a High Carbon Steel: Experiments and Modeling," *Acta Materialia*, vol. 217, p. 117176, 2021, doi: 10.1016/j.actamat.2021.117176.

[33] Y. Z. Zeng, K. M. Wu, F. Hu, and H. Zheng, "Effect of Partitioning of Quenching-Partitioning-Tempering Process on Microstructures and Hardness in High Carbon Steels," *Advanced Materials Research*, vol. 538–541, pp. 1053–1056, 2012, doi: 10.4028/www.scientific.net/AMR.538-541.1053.

[34] Y. Rong and N. Chen, "Multi-cycle quenching-partitioning-tempering (M Q-P-T) technique," 2013.

[35] Q. Hao, S. Qin, Y. Liu, X. Zuo, N. Chen, and Y. Rong, "Dynamic tensile behavior of novel

quenching-partitioning-tempering martensitic steel," *Heat Treatment and Surface Engineering*, vol. 1, no. 1–2, pp. 40–47, Apr. 2019, doi: 10.1080/25787616.2018.1560144.

[36] J. ping Lai, J. xin Yu, and J. Wang, "Effect of Quenching-Partitioning Treatment on the Microstructure, Mechanical and Abrasive Properties of High Carbon Steel," *International Journal of Minerals, Metallurgy and Materials*, vol. 28, no. 4, pp. 676–687, 2021, doi: 10.1007/s12613-020-2164-3.

[37] Y. Zhang *et al.*, "The Correlation Analysis of Microstructure and Tribological Characteristics of In Situ VCp Reinforced Iron-Based Composite.," *Materials (Basel, Switzerland)*, vol. 14, no. 15, Aug. 2021, doi: 10.3390/ma14154343.

[38] H. Zheng, K. M. Wu, O. Isayev, O. Hress, S. Yershov, and V. Tsepelev, "Effect of heat treatment parameters on the microstructure of quenching–partitioning–tempering steel," *Heat Treatment and Surface Engineering*, vol. 1, no. 1–2, pp. 83–86, Apr. 2019, doi: 10.1080/25787616.2018.1560168.

[39] N. Zhong *et al.*, "Effects of Compositional Inhomogeneity on the Microstructures and Mechanical Properties of a Low Carbon Steel Processed by Quenching-Partitioning-Tempering Treatment," *Crystals*, vol. 13, no. 1, 2023, doi: 10.3390/cryst13010023.

[40] A. Bhaduri, *Mechanical Properties and Working of Metals and Alloys*, vol. 264. Singapore: Springer Singapore, 2018.

[41] J. Pelleg, *Mechanical Properties of Materials*, 1st ed., vol. 190. Dordrecht: Springer Netherlands, 2013.

[42] Z. Huda, *Metallurgy for Physicists and Engineers*, 1st Editio. CRC Press, 2020.

[43] V. D. Kodgire and S. V. Kodgire, *Material Science and Metallurgy*. Everest Publishing House, 2018.

[44] D. Puspitasari, P. Puspitasari, M. Mustapha, and T. L. Ginta, "Effect of Heating Temperature, Holding Time and Stabilization Temperature on the Al-Foam Properties," *Journal of Mechanical Engineering Science and Technology (JMEST)*, vol. 7, no. 2, p. 147, 2023, doi: 10.17977/um016v7i22023p147.

[45] G. I. for Standardisation, "DIN 17100--Steels for General Structural Purposes," 1980.

[46] W. Wu *et al.*, "Mechanostructures: Rational mechanical design, fabrication, performance evaluation, and industrial application of advanced structures," *Progress in Materials Science*, vol. 131, p. 101021, Jan. 2023, doi: 10.1016/j.pmatsci.2022.101021.

[47] N. Aysal *et al.*, "Crystallization Kinetics: Relationship between Crystal Morphology and the Cooling Rate-Applications for Different Geological Materials," *Crystals*, vol. 13, no. 7. 2023, doi: 10.3390/cryst13071130.

[48] L. Wang and J. G. Speer, "Quenching and Partitioning Steel Heat Treatment," *Metallography, Microstructure, and Analysis*, vol. 2, no. 4, pp. 268–281, 2013, doi: 10.1007/s13632-013-0082-8.

[49] M. Carpio, J. Calvo, O. García, J. P. Pedraza, and J. M. Cabrera, "Heat Treatment Design for a QP Steel: Effect of Partitioning Temperature," *Metals*, vol. 11, no. 7. 2021, doi: 10.3390/met11071136.

[50] D. S. Smith, K. D. Clarke, and A. J. Clarke, "Leveraging chemical heterogeneity in steels heat treated to retain metastable austenite," *Scripta Materialia*, vol. 238, p. 115717, Jan. 2024, doi: 10.1016/j.scriptamat.2023.115717.

[51] R. Singh, "Heat Treatment of Steels," in *Applied Welding Engineering*, R. B. T.-A. W. E. (Second E. Singh, Ed. Elsevier, 2016, pp. 111–124.

[52] V. Javaheri *et al.*, "Rapid tempering of a medium-carbon martensitic steel: In-depth exploration of the microstructure – mechanical property evolution," *Materials & Design*, vol. 231, p. 112059, Jul. 2023, doi: 10.1016/j.matdes.2023.112059.

[53] ASTM International, "Standard test methods and definitions for mechanical testing of steel products A370-15," 2015.

[54] N. Uçak, A. Çiçek, and K. Aslantas, "Machinability of 3D printed metallic materials fabricated by selective laser melting and electron beam melting: A review," *Journal of Manufacturing Processes*, vol. 80, pp. 414–457, Aug. 2022, doi: 10.1016/j.jmapro.2022.06.023.

[55] K. Srivastava, A. A. Sinha, and R. Sahani, "Effect of heat treatment on hardness and toughness

of EN8 steel," *Materials Today: Proceedings*, vol. 42, pp. 1297–1303, 2021, doi: 10.1016/j.matpr.2020.12.1015.

[56] Y. H. Jo, Y. T. Choi, D. G. Kim, J. Han, and S. Lee, "Toughness behavior and deformation mechanisms in FCC-based Fe45Co30Cr10V10Ni5-xMnx high-entropy alloys: Insights from instrumented Charpy impact tests," *Journal of Materials Research and Technology*, vol. 30, pp. 1758–1767, May 2024, doi: 10.1016/j.jmrt.2024.03.211.

[57] A. Kumar, S. Sirohi, M. Singh, D. Fydrych, and C. Pandey, "Microstructure and mechanical properties of a dissimilar metal welded joint of Inconel 617 and P92 steel with Inconel 82 buttering layer for AUSC boiler application," *International Journal of Pressure Vessels and Piping*, vol. 209, p. 105196, Jun. 2024, doi: 10.1016/j.ijpvp.2024.105196.

[58] Z. Y. Hou, D. Wu, S. X. Zheng, X. L. Yang, Z. Li, and Y. B. Xu, "Effect of Holding Temperature on Microstructure and Mechanical Properties of High-Strength Multiphase Steel," *Steel Research International*, vol. 87, no. 9, pp. 1203–1212, Sep. 2016, doi: 10.1002/srin.201500331.

[59] E. Olorundaisi, T. Jamiru, and T. A. Adegbola, "Mechanical and microstructural evaluation of dual phase steel, quenched in bitumen and water at an intercritical temperature: effect of holding time," *Materials Research Express*, vol. 6, no. 11, p. 115606, Oct. 2019, doi: 10.1088/2053-1591/ab4747.

[60] E. Olorundaisi, T. Jamiru, and T. A. Adegbola, "Response surface modelling and optimization of temperature and holding time on dual phase steel," *Materials Today: Proceedings*, vol. 38, pp. 1164–1169, 2021, doi: 10.1016/j.matpr.2020.07.408.

[61] D. Xu, Y. Liu, J. Li, Q. Meng, and P. Li, "Microstructure Characterization and Mechanical Properties of TRIP-aided Steel under Rapid Heating for Different Holding Time," *Journal of Iron and Steel Research International*, vol. 23, no. 2, pp. 138–144, Feb. 2016, doi: 10.1016/S1006-706X(16)30025-5.

[62] O. Okwonna and O. M. Chima, "Investigation on the Interrelationship between the Chemical Composition, Heat Treatment Parameters and the Phase Transformation Process, Microstructure Evolution and the Mechanical Properties of Austempered Steel," *European Journal of Mechanical Engineering Research*, vol. 9, no. 2, pp. 1–12, 2022, doi: 10.37745/ejmer.2014.

[63] Y. Adamu, A. A. Adamu, Z. Salihu, and A. B. Musa, "Evaluation of combined heat treatment techniques of testing hardness and tensile strength of mild carbon steel commonly used in Nigeria," *Journal of Applied Sciences and Environmental Management*, vol. 23, p. 557, 2019, doi: 10.4314/jasem.v23i3.28.

[64] T. K. Ajiboye and A. Abdulsalam, "Mechanical Characteristics of Heat-Treated Medium Carbon Steel Quenched using Blending Different Types of Vegetable Oils," *International Journal of Engineering Materials and Manufacture*, vol. 4, pp. 146–153, 2019, doi: 10.26776/ijemm.04.04.2019.02.

[65] A. Bajželj and J. Burja, "Influence of Austenitisation Temperature and Time on Martensitic and Isothermal Bainite Phase Transformation of Spring Steel," *Metals*, vol. 12, no. 8, p. 1373, Aug. 2022, doi: 10.3390/met12081373.

[66] M. A. J. Somers and T. L. Christiansen, "Low temperature surface hardening of stainless steel," in *Thermochemical Surface Engineering of Steels*, E. J. Mittemeijer and M. A. J. B. T.-T. S. E. of S. Somers, Eds. Oxford: Elsevier, 2015, pp. 557–579.

[67] H. Chen *et al.*, "Atomic scale insights into the segregation/partitioning behaviour in as-sintered multi-main-phase Nd-Ce-Fe-B permanent magnets," *Journal of Alloys and Compounds*, vol. 846, p. 156248, Dec. 2020, doi: 10.1016/j.jallcom.2020.156248.

[68] A. Alabi, T. K. Ajiboye, and H. Olusegun, "Measuring the stress, strain and strain-rate in heat treated medium carbon steel samples and finding the constituited material related properties," *African Journal of Mathematics and Computer Science Research*, vol. 3, no. 3, pp. 38–48, 2010, doi: 10.5897/AJMCSR.9000078.

[69] V.K.Murugan and D. P. K. Mathews, "Effect of Tempering Behavior on Heat Treated Medium Carbon (C 35 Mn 75) Steel," *International Journal of Innovative Research in Science, Engineering and Technology*, vol. 2, no. 3, p. 2013, 2013.

[70] F. A. C. Nascimento, A. C. R. Guimarães, and C. D. Castro, "Comparative study on permanent deformation in asphalt mixtures from indirect tensile strength testing and laboratory wheel tracking," *Construction and Building Materials*, vol. 305, p. 124736, Oct. 2021, doi:

10.1016/j.conbuildmat.2021.124736.

[71] L. Kučerová, "The Effect of Two-Step Heat Treatment Parameters on Microstructure and Mechanical Properties of 42SiMn Steel," *Metals*, vol. 7, no. 12, 2017, doi: 10.3390/met7120537.

[72] A. Araoyinbo, "Low temperature heat treatment of steel and the effect of quenching on the strength and oxidation behaviour," *Mehran University Research Journal of Engineering and Technology*, vol. 42, p. 32, 2023, doi: 10.22581/muet1982.2301.04.

[73] M. Loffredo, "Measurement and modelling of Bauschinger effect for low-level plastic strains on AISI 4140 steel," *Procedia Structural Integrity*, vol. 8, pp. 265–275, 2018, doi: 10.1016/j.prostr.2017.12.028.

[74] W. Chen, D. Li, H. Cao, and Y. Chen, "Microstructure refinement and enhanced mechanical properties of wire arc additively manufactured RAFM steel via post heat treatments," *Journal of Materials Research and Technology*, vol. 29, pp. 4269–4285, 2024, doi: 10.1016/j.jmrt.2024.02.166.

[75] Q. Cui, S. Jiang, X. Lin, Y. Guo, H. Zhang, and B. Wen, "High-pressure quenching effect on martensitic transformation characteristics and mechanical properties of low-alloy medium-carbon steel," *Journal of Materials Research and Technology*, vol. 23, pp. 765–777, Mar. 2023, doi: 10.1016/j.jmrt.2023.01.051.

[76] Z. Xu, X. Guo, and Y. Zhao, "Experimental and theoretical study on axial stiffness of CFRP-bolted timber joints with slotted-in corrugated steel plates," *Construction and Building Materials*, vol. 416, p. 135001, Feb. 2024, doi: 10.1016/j.conbuildmat.2024.135001.

[77] S. Herbst, M. Schledorn, H. J. Maier, A. Milenin, and F. Nürnberger, "Process Integrated Heat Treatment of a Microalloyed Medium Carbon Steel: Microstructure and Mechanical Properties," *Journal of Materials Engineering and Performance*, vol. 25, no. 4, pp. 1453–1462, 2016, doi: 10.1007/s11665-016-2004-9.

[78] M. A. Farhad, Q. B. Jamali, A. S. Jamali, M. Ali, S. Ali, and A. Rao, "Analysis of Mechanical Properties of Medium Carbon Steel using various Heat Treatment Processes," *Quest Research Journal*, vol. 17, no. 2, pp. 61–65, 2019.

[79] X. Zhou *et al.*, "Cyclic quenching treatment doubles the Charpy V-notch impact energy of a 2.3 GPa maraging steel," *Journal of Materials Science & Technology*, vol. 209, pp. 311–328, Feb. 2025, doi: 10.1016/j.jmst.2024.05.026.

[80] C. Liang, W. Wang, H. He, and J. Zeng, "In situ observation of pearlite phase transition in high-carbon steel under different holding temperatures and cooling rates using confocal laser scanning microscope," *Journal of Materials Research and Technology*, vol. 23, pp. 6090–6100, Mar. 2023, doi: 10.1016/j.jmrt.2023.02.216.